

Inclusive Charged Current Neutrino Reactions:
Implications for Gauge Models with Heavy Quarks
and Right-Handed Currents

CARL H. ALBRIGHT* and R. E. SHROCK
Fermi National Accelerator Laboratory[†]
P. O. Box 500, Batavia, Illinois 60510

ABSTRACT

We analyze the predictions of several gauge theory models for deep inelastic neutrino reactions on both isoscalar and proton targets. In particular, we calculate y and W distributions, mean values of various kinematic quantities, and total cross sections. The effects of heavy quark production and the possible excitation of right-handed currents are discussed. In addition to the Weinberg-Salam and vector models, we study certain six-quark models which have parity-violating neutral currents. Estimates of effective heavy quark masses are presented for each model.

*Permanent address: Department of Physics, Northern Illinois University, DeKalb, Illinois 60115; work supported in part by National Science Foundation Grant No. MPS 75-05467.

I. INTRODUCTION

There is currently evidence for new phenomena in high energy deep inelastic charged current neutrino reactions. The available high energy data come from the Harvard-Pennsylvania-Wisconsin-Fermilab (HPWF)¹ and Caltech-Fermilab (CITF)² counter experiments, and from several collaborations using the 15' Fermilab bubble chamber. The latter include the Berkeley-Fermilab-Hawaii-Michigan (νH_2),³ Argonne-Carnegie-Mellon ($\bar{\nu}\text{H}_2$),⁴ Wisconsin-Berkeley-CERN-Hawaii ($\nu(\text{H}_2 + \text{Ne})$),⁵ and Fermilab-ITEP-Michigan ($\bar{\nu}(\text{H}_2 + \text{Ne})$)⁶ groups. The HPWF collaboration finds that as E, the (anti)neutrino energy increases beyond about 30 GeV, $\frac{d^2 \sigma^{\bar{\nu}\text{N}}}{dx dy}$ changes from the approximate $(1 - y)^2$ shape observed at low energy and acquires a flat component especially noticeable at high y. This effect is localized to the small x region, $x \lesssim 0.15$. Correspondingly, $\langle y \rangle^{\bar{\nu}\text{N}}$ and $R_{\text{ch}} = \sigma^{\bar{\nu}\text{N}} / \sigma^{\nu\text{N}}$ both increase substantially. Moreover, the distribution in invariant hadronic mass W for antineutrinos exhibits an enhancement at high W. The CITF data are consistent with HPWF on R_{ch} values. In both the HPWF and CITF data $d \sigma^{\nu\text{N}} / dy$ is consistent with being roughly flat and $\sigma^{\nu\text{N}}$ is observed to rise linearly with energy. The Fermilab νH_2 bubble chamber experiment confirms these two results. However, the $\bar{\nu}\text{H}_2$ experiment and the most recent results of the $\bar{\nu}(\text{H}_2 + \text{Ne})$ experiment do not show an anomalous y distribution. Hopefully this discrepancy will be resolved by the next generation of HPWF and CITF experiments and by increased statistics in the bubble chamber experiments.

A further important signal is the observation of dimuons by the HPWF and CITF groups and of μe events by CERN⁷ and the Fermilab $\nu(H_2 + Ne)$ experiment. These events are interpreted as indicating the weak production and semileptonic decay of hadrons with new quantum numbers, collectively called charm. The dilepton events may well be due to the excitation of currents involving different heavy quarks from those responsible for the reported anomalous y distribution and rise in $\langle y \rangle^{\bar{\nu}N}$ and R_{ch} . This would be the case, for example, if the b quark (see below) had a small semileptonic branching ratio. Accordingly, we shall concentrate here on the single muon data.

It is thus of interest to analyze the deep inelastic charged current data in the context of several different gauge theory models of weak interactions.⁸ In this paper the results of such an analysis are reported. We consider in addition to the Weinberg-Salam model⁹ several models with six quarks and right-handed currents. Results are presented for $d\sigma/dy$, $d\sigma/dW$, and the total cross sections for the reaction $\nu(\bar{\nu}) + N \rightarrow \mu^{\mp} + X$. We also comment on some of the corresponding results for the reaction $\nu(\bar{\nu}) + p \rightarrow \mu^{\mp} + X$ relevant to the bubble chamber experiments. Since our analysis is restricted to gauge theories we do not consider S, P, or T couplings. Finally, we do not discuss scaling deviations of the type predicted by asymptotically free gauge theories of strong interactions. A more detailed report on this work will be submitted for publication elsewhere.

II. GAUGE MODELS

We shall consider several gauge theory models of weak and electromagnetic interactions based on the gauge group $SU(2) \times U(1)$. It would be out of place to discuss these models in detail here; for this we refer the reader to the original papers. The relevant part of the lepton sector, viz. the $W_\lambda \bar{\mu} \gamma^\lambda (1 - \gamma_5) \nu_\mu + \text{h.c.}$ term in the Lagrangian, (with W_λ the W boson field) is the same for all of these models. The quarks are arranged in doublets and singlets; of course, only the doublets are involved in charged current transitions. Table 1 shows the doublet structure in the models considered here.

In the Weinberg-Salam (W-S) theory⁹ with the necessary Glashow-Iliopoulos-Maiani modification¹⁰ to avoid strangeness changing neutral currents there are four "flavors" of (tricolored) quarks: the three light quarks u , d , and s , and an additional heavy one, c . These are placed in two left-handed doublets as shown in Table 1. The Cabibbo rotated quarks are given by

$$d_\theta = d \cos \theta_C + s \sin \theta_C \tag{2.1}$$

$$s_\theta = -d \sin \theta_C + s \cos \theta_C$$

where θ_C is the Cabibbo angle. A second theoretically appealing model was proposed by Kingsley, Treiman, Wilczek and Zee¹¹ and Fritzsche, Gell-Mann, and Minkowski,¹² De Rujula, Georgi, and Glashow,¹³ and Pakvasa,

Pilachowski, Simmons, and Tuan.^{8, 14} In this theory there are six flavors of quarks, u, d, s, c, and two additional heavy ones t and b, arranged symmetrically in three left-handed and three right-handed doublets, as shown in Table 1. The upper member of each doublet has electric charge $Q = 2/3$, the lower member $Q = -1/3$. This model is called the vector (V) model since both the neutral current and, in the asymptotic region where quark masses are negligible, also the charged current are pure vector. Recent HPWF and CTF neutral current data appear to rule out a vector neutral current. It is nevertheless of some interest to see how well the vector model fares in explaining the charged current data.

Another class of six quark models, considered by Barnett¹⁵ and by Gürsey, Sikivie, and Ramond,¹⁶ contains two $Q = 2/3$ quarks and four $Q = -1/3$ ones. These are placed in two left-handed and two right-handed doublets, and in singlets, in such a way that the neutral current is not purely vector. We shall consider in particular two versions --(B) and (C) in the authors' notation, of the Gürsey-Sikivie (G-S) model. Table 1 shows how the six quarks u, d, s, c, b, and b' are placed in two left-handed and two right-handed doublets. The right-handed b and b' quarks are rotated according to

$$b_{\phi_R} = b_R \cos \phi + b'_R \sin \phi \tag{2.2}$$

and

$$b'_{\phi_R} = -b_R \sin \phi + b'_R \cos \phi,$$

where b'_{ϕ_R} is a singlet. In the G-S (C) model the left-handed u and c quarks are rotated according to

$$u_{\alpha_L} = u_L \cos \frac{\alpha}{2} + c_L \sin \frac{\alpha}{2} \quad (2.3)$$

$$c_{\alpha_L} = -u_L \sin \frac{\alpha}{2} + c_L \cos \frac{\alpha}{2}$$

while the following rotated $Q = -1/3$ quarks also appear in doublets:

$$d_{\alpha_L} = d_L \cos \frac{\alpha}{2} + b_L \sin \frac{\alpha}{2} \quad (2.4)$$

$$b'_{\alpha_L} = -s_L \sin \frac{\alpha}{2} + b'_L \cos \frac{\alpha}{2}$$

In the (C) version, $\tan^2 \alpha/2 = \tan^2 \theta_C$ so that the $d \rightarrow c$ transition is suppressed by only $\tan \theta_C$ rather than $\tan^2 \theta_C$. Moreover, cancellation of the cross terms does not occur via a GIM mechanism and consequently above b and b' thresholds the neutral current becomes flavor-changing. For reference, the Barnett model has the right-handed doublets $\begin{pmatrix} u \\ d' \end{pmatrix}_R, \begin{pmatrix} c \\ s' \end{pmatrix}_R$; d'_R corresponds to b_R but in contrast to the G-S models, the c_R quark is coupled to another heavy quark s'_R rather than to s_R . In both the G-S and the Barnett models the $u \rightarrow b$ transition is by far the most important V + A effect since it is of valence strength. Indeed a minimal, albeit rather asymmetric model with five quarks has been introduced by Achiman, Koller, and Walsh (AKW).¹⁷ This model includes just one right-handed

doublet $\begin{pmatrix} u \\ b \end{pmatrix}_R$. (We have actually generalized the model slightly as indicated in Table 1 by allowing for u-c mixing.) For $\cos \phi = 1$ this model gives predictions which are similar to those of the Barnett and G-S models.

In all these models the charged current is given simply by

$$J_{\mu}^{\pm} = \sum_L \bar{\Psi}_L \tau_{\pm} \gamma_{\mu} (1 - \gamma_5) \Psi_L + \sum_R \bar{\Psi}_R \tau_{\pm} \gamma_{\mu} (1 + \gamma_5) \Psi_R \quad (2.5)$$

where the first sum runs over the left-handed doublets and the second one over the right-handed doublets if any. Having thus specified the relevant structure of the gauge models to be considered we shall next proceed with the calculations.

III. CALCULATIONS

The neutrino reactions to be considered are

$$\nu(\bar{\nu}) + N \rightarrow \mu^{\mp} + X \quad (3.1)$$

and

$$\nu(\bar{\nu}) + p \rightarrow \mu^{\mp} + X$$

where N denotes an isoscalar nucleon target. Such a target is provided to a good approximation by the HPWF and CITEF experiments and by heavy liquid bubble chamber experiments. An ideal proton target is provided by the H₂ bubble chamber experiments.

The differential cross section for the reaction of Eq. (3.1a) can be written as

$$\frac{\partial^2 \sigma^{(\nu, \bar{\nu})N}}{\partial x \partial y} = \frac{G^2 ME}{\pi} \left[xy^2 F_1^{(\nu, \bar{\nu})N} + (1-y) F_2^{(\nu, \bar{\nu})N} \mp y(1-\frac{y}{2}) x F_3^{(\nu, \bar{\nu})N} \right], \quad (3.2)$$

where $x = Q^2/2M\nu$ and $y = E - E'$ are the usual scaling variables, with $q^2 = -Q^2$ the momentum transfer squared, $E(E')$ the lab energies of the incident (scattered) lepton, and $\nu = q \cdot p/M = E - E'$ the lab energy transfer. The same equation applies, with appropriate changes in the F_i , to the $(\nu, \bar{\nu})p$ reactions (2b). According to the Bjorken scaling hypothesis, as $Q^2 \rightarrow \infty$ and $\nu \rightarrow \infty$ with x fixed the (dimensionless) structure functions $F_i = F_i(Q^2, \nu)$ scale, i. e. are functions only of x . In the parton model this follows naturally since the lepton is viewed as scattering elastically off free quarks with negligible masses. Elementary kinematics then implies that for a given q^2 and ν such a scattering process can take place only off a quark carrying a fraction $x = Q^2/2M\nu$ of the initial nucleon momentum.

However, when a heavy quark is produced in the transition $q_i (+ W^\pm) \rightarrow q_j$ the dependence of the structure functions on the kinematic variables is not so simple. An analysis of the quark mass dependence of the operator product expansion of two currents which is relevant for deep inelastic leptonproduction shows that for the case of a light quark to heavy quark transition the F_i are functions of an effective scaling variable z_j given by¹⁸

$$z_j = x + \frac{m_j^2}{2MEy} \quad (3.3)$$

Here m_j represents an effective mass appropriate to the heavy produced quark. A heuristic parton model argument can also be used to derive the result (4). Again, elastic scattering kinematics implies that if the incident (light) quark carries a fraction z_j of the total nucleon momentum, in the infinite momentum frame, then $(z_j p + q)^2 = m_j^2$, which yields Eq. (4). Since quarks presumably do not exist as asymptotic states it is not possible to define a quark mass, e.g. as the pole of the renormalized propagator. For the purposes of our computations m_j will be treated as a phenomenological constant.

In the case of heavy quark production, the Callan-Gross relation for the allowed transition $q_i \rightarrow q_j$ or $\bar{q}_i \rightarrow \bar{q}_j$ is

$$F_2(z_j) = 2 z_j F_1(z_j) \tag{3.4}$$

Similarly, the relation between F_2 and F_3 is

$$-z_j F_3(z_j) = B_{ij} F_2(z_j) \tag{3.5}$$

where

$$B_{ij} = \begin{cases} +1 \text{ for } (q_i)_L \rightarrow (q_j)_L \\ \text{or } (\bar{q}_i)_R \rightarrow (\bar{q}_j)_R \\ -1 \text{ for } (q_i)_R \rightarrow (q_j)_R \\ \text{or } (\bar{q}_i)_L \rightarrow (\bar{q}_j)_L \end{cases} \tag{3.6}$$

That is, $B_{ij} = +1$ for negative helicity quarks and -1 for positive helicity quarks. Thus the contribution to the differential cross section of the light to heavy quark transition $q_i \rightarrow q_j$ is

$$\frac{\partial^2 \sigma^{\nu, \bar{\nu}}}{\partial x \partial y} (i \rightarrow j) = \frac{G^2 ME}{\pi} \left[\left(1 - y + \frac{xy^2}{2z_j} \right) \pm \frac{x}{z_j} y \left(1 - \frac{y}{2} \right) B_{ij} \right] F_2^{(i \rightarrow j)}(z_j) \quad (3.7)$$

where

$$F_2^{(i \rightarrow j)}(z_j) = 2 z_j u_i(z_j) \quad (3.8)$$

with $u_i(z_j)$ the parton probability distribution function for a quark of flavor i to have momentum z_j . The total cross section is obtained in the usual way by assuming incoherent scattering and hence additivity of individual quark cross sections.

In order to carry out subsequent integrations over z , y , or x to obtain various partially integrated distributions one must also take into account the fact that associated with the weak production of a new flavor quark is the production of physical hadrons carrying new flavor quantum numbers. In order for this latter process to occur, the hadronic invariant mass W must be larger than a threshold value W_j , where $j = c, b, t$ etc. Consequently, there is implicitly a factor $\theta(W - W_j)$ multiplying the right-hand side of Eq. (3.7).

The parton distributions used in our calculations incorporate the conventional SU(3) symmetric sea:

$$u(x) = u_V(x) + \xi(x) \quad (3.9)$$

$$d(x) = d_V(x) + \xi(x) \quad (3.10)$$

$$\bar{u}(x) = \bar{d}(x) = s(x) = \bar{s}(x) = \xi(x) \quad (3.11)$$

with heavy quarks absent. We have used a parton parametrization due to R. D. Field¹⁹ which has a sea quark distribution $\xi(x) \propto x^{-1}(1-x)^7$ for $x \rightarrow 1$ and gives a satisfactory fit to SLAC electroproduction data and low energy ($E < 30$ GeV) neutrino data. It has a 3.5% sea content, the latter being defined here as

$$\frac{\int_0^1 2x \xi(x) dx}{\int_0^1 x [u_V(x) + d_V(x)] dx} \quad (3.12)$$

At low energy the field parton parametrization yields $\langle y \rangle^{\nu N} \approx 0.50$, $\langle y \rangle^{\bar{\nu} N} \approx 0.30$, $\langle x \rangle^{\nu N} \approx 0.26$, $\langle x \rangle^{\bar{\nu} N} \approx 0.24$, $\langle Q^2/E \rangle^{\nu N} \approx 0.24$ GeV, $\langle Q^2/E \rangle^{\bar{\nu} N} \approx 0.12$ GeV, and $\sigma^{\bar{\nu} N} / \sigma^{\nu N} \approx 0.40$. For comparison we have also used the Pakvasa-Parashar-Tuan (PPT)²⁰ parametrization, which has a sea quark distribution characterized by a less rapid decrease with x : $\xi(x) = 0.1 x^{-1} (1-x)^{3.5}$. This gives a sea content of 5.5%. The u and d quark distributions are quite similar in both of these

parametrizations. The effects which we observe in the models with right handed valence transitions are thus not sensitively dependent upon the differences between the field and PPT parton parametrizations. The small contributions of heavy quark production off sea quarks are somewhat enhanced in the PPT parametrization.

IV. RESULTS AND CONCLUSIONS

For the numerical results to be presented here we have chosen the following values of effective quark masses, in units of GeV: $m_c = 1.5$ in all models, $m_b = 4$, $m_t = 5$ in the vector model, and $m_b = 3.5$, $m_{b'} = 6$ in the G-S(B) and G-S(C) models. The corresponding thresholds in hadronic invariant mass have been chosen as $W_j = m_j + 1$, $j = c, b, t, b'$. We have also considered other choices of effective quark masses and threshold values of W . Finally, in the G-S(B) and G-S(C) models the value $\cos^2 \phi = \frac{1}{2}$ has been used. We shall concentrate here on the most striking effects of heavy quark production and the excitation of right handed currents, which, aside from dimuons, are mostly strongly manifest in antineutrino reactions.

In Fig. 1 we show the normalized y distribution for the reaction $\nu + N \rightarrow \mu^+ + X$ at $E = 30$ GeV. Fig. 2 depicts the y distribution for x integrated only from 0 to 0.1. (For economy of notation the same symbol $\frac{1}{\sigma} \frac{d\sigma}{dy} \nu N$ is used for both graphs; note in particular that in Fig. 2, σ refers to the cross section for x integrated only over the

interval 0 to 0.1. Figs. 3 and 4 show the same quantities at $E = 80$ GeV. Let us consider first the W-S model. There is of course always a small flat component arising from the $\bar{d} \rightarrow \bar{u}$ and $\bar{s} \rightarrow \bar{u}$ transitions. The latter of these is negligible since it not only occurs off sea quarks but also is suppressed by the factor $\sin^2 \theta_C$. As E passes the threshold for c quark production the $\bar{s} \rightarrow \bar{c}$ (and negligible $\bar{d} \rightarrow \bar{c}$) transition occurs, again giving a flat contribution to $\frac{d\sigma^{\bar{\nu}N}}{dy}$. This effect is more noticeable at small x because it involves sea quarks. Furthermore for energies not too far beyond threshold, in order to maximize W sufficiently to produce heavy quarks and physical hadrons with new flavors, x is kinematically forced to be small (and y large) by the relation $W^2 - M^2 = 2MEy(1 - x)$. Given the values of m_c and W_c which we use, the effect has already set in before 30 GeV and, as one can see from Figs. 1 and 3, it does not increase between 30 and 80 GeV. Because such a sea effect is rather small the total $\frac{d\sigma^{\bar{\nu}N}}{dy}$ retains an approximate $(1 - y)^2$ form.

The behavior of $\frac{d\sigma^{\bar{\nu}N}}{dy}$ as a function of energy is quite different in the other three models considered, primarily because of the onset of the $V + A$ $u \rightarrow b$ (and/or b') transition. This transition occurs off valence quarks and, neglecting small contributions due to sea quarks, for E far above threshold, it changes $\frac{d\sigma^{\bar{\nu}N}}{dy}$ from $\propto (1 - y)^2$ to $\propto [1 + (1 - y)^2]$. In the naive valence quark model, $\langle y \rangle^{\bar{\nu}N}$ would thus change from $\frac{1}{4}$ to $\frac{7}{16}$ and $\sigma^{\bar{\nu}N}$ would increase by a factor of four, the $V + A$ term being enhanced by a factor of three relative to the $V - A$ term. It is important

to note that although the $V + A \ u \rightarrow b$ transition occurs off a valence quark, at energies not asymptotically far above threshold, it contributes mainly at small x , simply because of the kinematic necessity of achieving $W > W_{Th}$. Stated alternatively, the fact that the flattening of $\frac{d\sigma}{dy} \bar{\nu}N$ observed by HPWF requires valence strength right-handed currents (see below) and the fact that it occurs most strongly at small x do not constitute a paradox. Although x is forced to be small, the real quark momentum fraction z is not small; indeed $z > \frac{m_q}{2MEy}$. For example, with $m_b = 4$ GeV, $E = 40$ GeV, $y = 0.6$, $z_b > 0.35$. From Figs. 1 and 3 one can observe immediately that in the vector, G-S (B), and G-S (C) models $\frac{d\sigma}{dy} \bar{\nu}N$ is considerably flatter for $E = 80$ than it is for $E = 30$ GeV. In the G-S (B) model, for example, as E increases through the values 10, 30, 80, and 120 GeV, respectively, $\frac{1}{\sigma} \frac{d\sigma}{dy} \bar{\nu}N$ ($y = 1$) takes on the values 0.17, 0.41, 0.69, and 0.78, respectively. One can see the evolution of the threshold shoulder structure in Figs. 1 to 4. As expected, the position of the shoulder moves to lower y as E increases, and, at a given E , it occurs at lower y in the $\frac{d\sigma}{dy}$ ($x < .1$) plots than in the full $\frac{d\sigma}{dy}$ plots.

We do not show the results for $\frac{d\sigma}{dy} \nu N$ since experimentally it is not as sensitive to the onset of heavy quark production as $\frac{d\sigma}{dy} \bar{\nu}N$ is. The changes in $\frac{d\sigma}{dy}$ depend primarily on whether there is a right-handed $\begin{pmatrix} t \\ d \end{pmatrix}_R$ doublet in a given model. In the W-S and G-S(B) and (C) models there is no such doublet, and accordingly $\frac{d\sigma}{dy} \nu N$ remains quite flat with increasing energy. In contrast, in the vector model, the onset of

the V+A $d \rightarrow t$ transition gives rise to a valence strength $(1-y)^2$ term in $\frac{d\sigma^{\nu N}}{dy}$ so that far above threshold, $\frac{d\sigma}{dy} \sim [1+(1-y)^2]$. However at non-asymptotic energies the kinematic preference for high y to produce heavy quarks combines with the $1+(1-y)^2$ shape of the heavy quark y distribution to yield a $\frac{d\sigma^{\nu N}}{dy}$ with a maximum at an intermediate value, $y \sim 0.5$. Hence $\langle y \rangle^{\nu N}$ deviates only very slightly from its low energy value of ~ 0.5 . The experimental data are consistent with $\frac{d\sigma^{\nu N}}{dy}$ being flat but do not discriminate among different models.

There are two kinematic quantities which serve to characterize the y distribution, viz. $\langle y \rangle$ and an effective B parameter, the latter being defined here by the equation

$$\frac{d\sigma^{(\nu, \bar{\nu})N}}{dy} \propto \left[\left(1 - y + \frac{y^2}{2} \right) \pm y \left(1 - \frac{y}{2} \right) B \right]. \quad (4.1)$$

We have chosen this definition of B because it is the one used by the experimentalists, who fit their measured y distributions to Eq.(4.1). It should be recalled, however, that in the presence of heavy quark production the y dependence of the differential cross section is given by Eq. (3.7) summed over all possible quark transitions and is not so simple as the form (4.1). In particular, the x and y dependences no longer factorize and the parton distribution functions themselves depend on y , through the variable z . In order to compare with

experimental determinations of B we, too, have fitted our y distributions to Eq. (4.1). The results are shown in Figs. 5 and 6 for the fits to $\frac{1}{\sigma} \frac{d\sigma^{\bar{\nu}N}}{dy}$ and $\frac{1}{\sigma(x < 0.1)} \frac{d\sigma^{\bar{\nu}N}}{dy}$ ($x < 0.1$) respectively. For reference, the HPWF data give (for $x < 0.6$) $B^{\bar{\nu}N} = 0.94 \pm 0.09$ for $10 < E < 30$ GeV and $B^{\bar{\nu}N} = 0.41 \pm 0.13$ for $E > 70$ GeV. At asymptotic energies models with a $V+A$ $u \rightarrow b$ transition have, neglecting small sea contributions $B^{\bar{\nu}N} = 0$. It is evident from Figs. 5 and 6 that the fitted values of $B^{\bar{\nu}N}$ are negative in the range $E \geq 80$ GeV, i. e. correspond to $\frac{d\sigma}{dy}$ closer to being flat than $1 + (1 - y)^2$. This is simply a reflection of the shoulder structure in $\frac{d\sigma}{dy}$ and indeed at higher energies, as the shoulder moves back to $y = 0$ the calculated $B^{\bar{\nu}N}$ values do approach the vicinity of zero.

Next, Fig. 7 shows the results of our calculation of $\langle y \rangle^{\nu N}$ and $\langle y \rangle^{\bar{\nu}N}$. In the case of $\langle y \rangle^{\nu N}$, as for $\frac{d\sigma}{dy}$, there is very little change in the W-S, G-S(B), and G-S(C) models. At very high energies $\langle y \rangle^{\nu N}$ in the vector model does indeed fall to 0.438, close to the value of $7/16$ predicted by the valence quark model. The curves for $\langle y \rangle^{\bar{\nu}N}$ in the various models largely reflect the trend in $\frac{1}{\sigma} \frac{d\sigma}{dy}$ illustrated by Figs. 1 and 3. For comparison, the HPWF values of $\langle y \rangle^{\bar{\nu}N}$ rise from ~ 0.28 at low energies to $\sim 0.37 \pm 0.02$ at $E = 60$ GeV and $\sim 0.40 \pm 0.03$ for $80 \leq E \leq 100$. The W-S model cannot reproduce this rise in $\langle y \rangle^{\bar{\nu}N}$, just as it could not account for the flattening of $\frac{d\sigma^{\bar{\nu}N}}{dy}$ and decrease of $B^{\bar{\nu}N}$. In the vector and G-S(B, C) models it is possible to reproduce

this growth in $\langle y \rangle^{\bar{\nu}N}$ by taking $m_b = 5$ GeV, $W_b = 6$ GeV (and retaining the values of m_b , and W_b , in the G-S(B) and G-S(C) models). At still higher energies the calculated curves in these three models go above the measured values of $\langle y \rangle^{\bar{\nu}N}$, which fall to 0.36 ± 0.05 at $E = 140$ GeV.

The production of heavy quarks and hadrons with commensurately higher thresholds in W has the effect of skewing the W distribution toward the high end. In Figs. 8 and 9 we present curves for $\frac{1}{\sigma} \frac{d\sigma^{\bar{\nu}N}}{dW}$ at $E = 30$ and 80 GeV in the four models studied. At $E = 30$ GeV in the three models with b, t and/or b' quarks there is a shoulder developing around $W = 5-6$ GeV; at $E = 80$ GeV this has grown into a maximum at $W \sim 8$ GeV. This general pattern of enhancement of the higher part of the W distribution may help to account for the enhancement observed in the HPWF data, especially in the 50-100 GeV energy bin.

Finally, Fig. 10 indicates the deviation of the total cross sections from the scaling behavior of a linear growth in E . The striking increase in $\frac{\sigma^{\bar{\nu}N}}{E}$ for the G-S(C) model is a result of the V-A $d \rightarrow c$ transition which occurs because of the mixing of the u and c quarks in $u_{\alpha L} = u_L \cos \frac{\alpha}{2} + c_L \sin \frac{\alpha}{2}$. This increase is not in very good agreement with the HPWF and CITF data, which show that $\frac{\sigma^{\bar{\nu}N}}{E}$ is constant (to within the experimental errors of $\sim 15\%$). The ratio $\frac{\sigma^{\bar{\nu}N}}{\sigma^{\nu N}}$ is shown next, in Fig. 11. The W-S model curve disagrees with the reported results of the HPWF and CITF experiments. In contrast the vector, G-S(B) and G-S(C) models, are consistent with the rise in

R_{ch} as reported by the HPWF group, from 0.38 ± 0.06 for $E < 30$ GeV to $0.6 - 0.7$ in the region $50 \leq E \leq 100$ GeV. The CITF data similarly give $R_{\text{ch}} \approx 0.50$ at $E \sim 50$ GeV and 0.69 at $E \sim 150$ GeV. Finally, in Fig. 12 we plot $\frac{\sigma_{\bar{\nu}N}}{\sigma_{\nu N}}$ as a function of E . It will be interesting to compare the predictions of the various models with experiment when accurate measurements of $\frac{\sigma_{\bar{\nu}N}}{\sigma_{\nu N}}$ and $\frac{\sigma_{\bar{\nu}p}}{\sigma_{\nu p}}$ become available from bubble chamber experiments.

In conclusion, then, we find that the HPWF and CITF data seem to require the excitation at high energy of right handed valence strength currents involving light to heavy quark transitions. The Weinberg-Salam model is not able to explain these results of the experiments. However, the vector and Gürsey-Sikivie (B) and (C) models, all of which have a $V+A$ $u \rightarrow b$ transition, are, with appropriate choices of effective quark masses and physical thresholds, able to account, at least qualitatively, for the changes in $\frac{d\sigma_{\bar{\nu}N}}{dy}$ and the rise in $\langle y \rangle_{\bar{\nu}N}$ and R_{ch} .

ACKNOWLEDGMENTS

We would like to thank A. Benvenuti, A. Bodek, D. Buchholtz, D. Cline, B. W. Lee, T. Y. Ling, A. K. Mann, F. Merrit, F. Nezrick, C. Quigg, and W. Scott for helpful discussions.

FOOTNOTES AND REFERENCES

- ¹For reviews of the HPWF data see (in chronological order) D. Cline, talk given at the Palermo Conference (June 1975); C. Rubbia, in the Proceedings of the 1975 International Symposium on Lepton and Photon Interactions at High Energies, Stanford, ed. W. T. Kirk (Stanford; SLAC, 1976); D. Cline, talk delivered at the Irvine Conference (December, 1975); A. K. Mann, talk given at "Orbis Scientiae," Coral Gables (January, 1976); T. Y. Ling and P. Wanderer in the Proceedings of the International Conference on the Production of Particles with New Quantum Numbers, Madison, Wisconsin (April, 1976). Recent HPWF data on the high y anomaly, $\sigma^{\bar{\nu}N}/\sigma^{\nu N}$, invariant mass distributions, and neutral currents can be found, respectively, in HPWF preprints No. 76/1, 76/2, 76/3, and 76/4.
- ²For reviews of the CITEF data, see B. C. Barish in the Proceedings of the 1975 Symposium on Lepton and Photon Interactions at High Energies, Stanford, op. cit.; F. Sciulli, in Particles and Fields 1975, eds. H. Lubatti and P. Mockett (Seattle, University of Washington Press, 1976); F. Sciulli in Orbis Scientiae, Coral Gables (January, 1976); A. Bodek, talk given at the Rencontre de Moriond Flaine (1976); B. C. Barish, talk given at the Vanderbilt Conference (April, 1976), Caltech Report No. CALT 68-544; L. Stutte, in the Proceedings of the Madison Conference, op. cit. The relevant data

from these papers are the values for α , the fraction of positive helicity coupling. The "non-scaling" fit gives $\alpha = 0.17^{+0.13}_{-0.11}$ at $E \approx 50$ GeV and $\alpha = 0.32^{+0.18}_{-0.15}$ at $E \approx 150$ GeV. These values of α yield directly the values of R quoted in the text, $R = 0.50^{+0.15}_{-0.12}$ at $E \approx 50$ GeV and $R = 0.69^{+0.26}_{-0.22}$ at $E \approx 150$ GeV. The CITF group has also fitted its data to the Barnett model (Ref. 15) and found reasonable agreement; the b quark mass is determined to be $m_b = 5 \pm 1.5$ GeV.

³J. P. Berge et al., Phys. Rev. Lett. 36, 639 (1976).

⁴M. Derrick et al., Phys. Rev. Lett. 36, 936 (1976).

⁵J. Van Krogh et al., Phys. Rev. Lett. 36, 710 (1976).

⁶W. Scott, talk delivered at the Vanderbilt Conference (April, 1976).

Upon further analysis of the data, the Fermilab-ITEP-Michigan group has obtained results which differ from those presented at the Vanderbilt Conference and do not indicate a strong anomalous y distribution setting in at high energy.

⁷J. Blietschau et al., Phys. Lett. 60B, 207 (1976).

⁸Similar calculations have been done by S. Pakvasa, L. Pilachowski, W. A. Simmons, and S. F. Tuan, Hawaii preprint (December, 1975); R. M. Barnett, Harvard preprint (February, 1976); Phys. Rev. Lett. 36, 1163 (1976); and V. Barger, T. Weiler, and R. Phillips, Wisconsin preprint (April, 1976).

- ⁹S. Weinberg, Phys. Rev. Lett. 19, 1264 (1967), ibid. 27, 1688 (1971).
A. Salam, in Elementary Particle Theory, ed. N. Svartholm
(Stockholm: Almquist and Wiksell, 1969), p. 367.
- ¹⁰S. L. Glashow, J. Illiopoulos, and L. Maiani, Phys. Rev. D2,
1285 (1970).
- ¹¹F. Wilczek, A. Zee, R. Kingsley, and S. Treiman, Phys. Rev.
D12, 2768 (1975).
- ¹²H. Fritzsch, M. Gell-Mann, and P. Minkowski, Phys. Lett. 59B,
256 (1975).
- ¹³A. De Rújula, H. Georgi, and S. L. Glashow, Phys. Rev. D12,
3589 (1975).
- ¹⁴The vector models originally proposed by De Rújula et al. (Phys.
Rev. Lett. 35, 69 (1975)) and Pakvasa, Simmons and Tuan (Phys.
Rev. Lett. 35, 702 (1975)) contained a $\begin{pmatrix} c \\ d \end{pmatrix}_R$ doublet which is ruled
out by experiment. The De Rújula et al. model of Ref. 13 and the
Pakvasa et al. model of Ref. 8 amended this problem.
- ¹⁵R. M. Barnett, Phys. Rev. Lett. 34, 41 (1975); Phys. Rev. D11,
3246 (1975).
- ¹⁶F. Gürsey and P. Sikivie, Phys. Rev. Lett. 36, 775 (1976);
P. Ramond, Caltech preprint CALT-68-540, to be published.
- ¹⁷Y. Achiman, K. Koller, and T. Walsh, Phys. Lett. 58B, 261 (1975).
This model has also been discussed by B. W. Lee at the Washington
APS Meeting (April, 1976).

¹⁸H. Georgi and H. D. Politzer, Phys. Rev. Lett. 36, 1281 (1976);

Harvard preprint, 1976, and references therein.

¹⁹R. D. Field, Caltech report, unpublished.

²⁰S. Pakvasa, D. Parashar, and S. F. Tuan, Phys. Rev. D10, 2124

(1974); see also J. Okada, S. Pakvasa, and S. F. Tuan, Hawaii preprint.

Table I. Left-handed and right-handed doublet structure for the $SU(2) \otimes U(1)$ models considered in the text.

Model	Left-handed Doublets	Right-handed Doublets
Weinberg-Salam	$\begin{pmatrix} u \\ d_{\theta_L} \end{pmatrix}, \begin{pmatrix} c \\ s_{\theta_L} \end{pmatrix}$	-----
Vector	$\begin{pmatrix} u \\ d_{\theta_L} \end{pmatrix}, \begin{pmatrix} c \\ s_{\theta_L} \end{pmatrix}, \begin{pmatrix} t \\ b \end{pmatrix}_L$	$\begin{pmatrix} u \\ b \end{pmatrix}_R, \begin{pmatrix} c \\ s \end{pmatrix}_R, \begin{pmatrix} t \\ d \end{pmatrix}_R$
Achiman, Koller, Walsh	$\begin{pmatrix} u \\ d_{\theta_L} \end{pmatrix}, \begin{pmatrix} c \\ s_{\theta_L} \end{pmatrix}$	$\begin{pmatrix} u \\ b \end{pmatrix}_R$
Gürsey-Sikivie (B)	$\begin{pmatrix} u \\ d_{\theta_L} \end{pmatrix}, \begin{pmatrix} c \\ s_{\theta_L} \end{pmatrix}$	$\begin{pmatrix} u \\ b_{\phi} \end{pmatrix}_R, \begin{pmatrix} c \\ s \end{pmatrix}_R$
Gürsey-Sikivie (C)	$\begin{pmatrix} u_{\alpha} \\ d_{\alpha_L} \end{pmatrix}, \begin{pmatrix} c_{\alpha} \\ b_{\alpha_L} \end{pmatrix}$	$\begin{pmatrix} u \\ b_{\phi} \end{pmatrix}_R, \begin{pmatrix} c \\ s \end{pmatrix}_R$

FIGURE CAPTIONS

- Fig. 1: $\frac{1}{\sigma} \frac{d\sigma^{\bar{\nu}N}}{dy}$ at $E = 30$ GeV. The four curves represent the predictions of the Weinberg-Salam (W-S), vector (V), and Gürsey-Sikivie (G-S) (B) and (C) models.
- Fig. 2: $\frac{1}{\sigma} \frac{d\sigma^{\bar{\nu}N}}{dy}$ for $x < 0.1$ and $E = 30$ GeV. The cross section σ used to normalize the y distribution is calculated for x intergrated between 0 and 0.1.
- Fig. 3: $\frac{1}{\sigma} \frac{d\sigma^{\bar{\nu}N}}{dy}$ at $E = 80$ GeV.
- Fig. 4: $\frac{1}{\sigma} \frac{d\sigma^{\bar{\nu}N}}{dy}$, as in Fig. (2) but at $E = 80$ GeV.
- Fig. 5: $B^{\bar{\nu}N}$ as a function of E .
- Fig. 6: $B^{\bar{\nu}N}$ as calculated from the $x < 0.1$ y distribution, as a function of E .
- Fig. 7: $\langle y \rangle^{\nu N}$ and $\langle y \rangle^{\bar{\nu}N}$ as functions of E .
- Fig. 8: $\frac{1}{\sigma} \frac{d\sigma^{\bar{\nu}N}}{dW}$ at $E = 30$ GeV.
- Fig. 9: $\frac{1}{\sigma} \frac{d\sigma^{\bar{\nu}N}}{dW}$ at $E = 80$ GeV.
- Fig. 10: $\sigma^{\nu N}/E$ and $\sigma^{\bar{\nu}N}/E$, as functions of E .
- Fig. 11: $\sigma^{\bar{\nu}N}/\sigma^{\nu N}$.
- Fig. 12: $\sigma^{\bar{\nu}P}/\sigma^{\nu P}$.

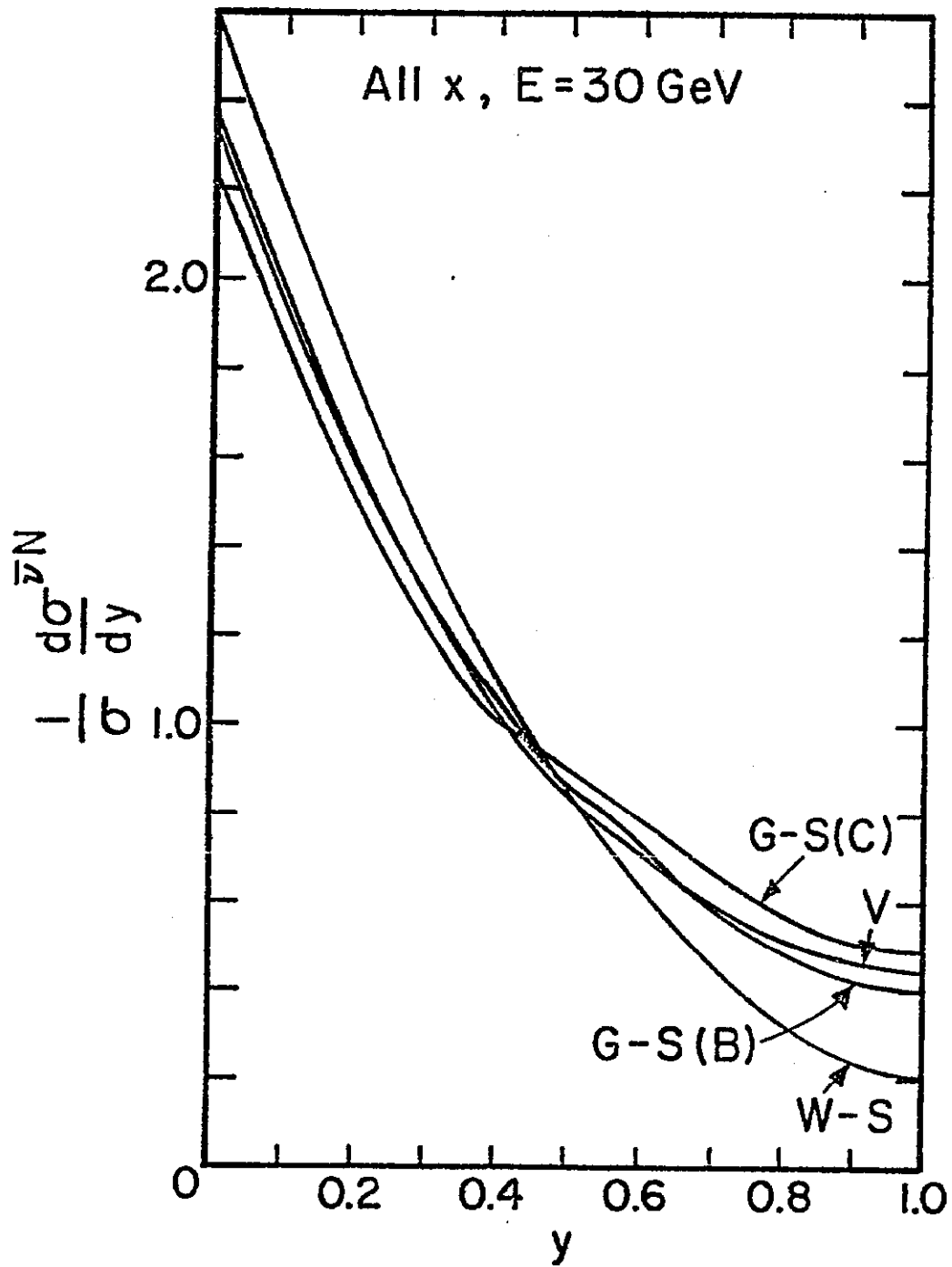


Fig. 1

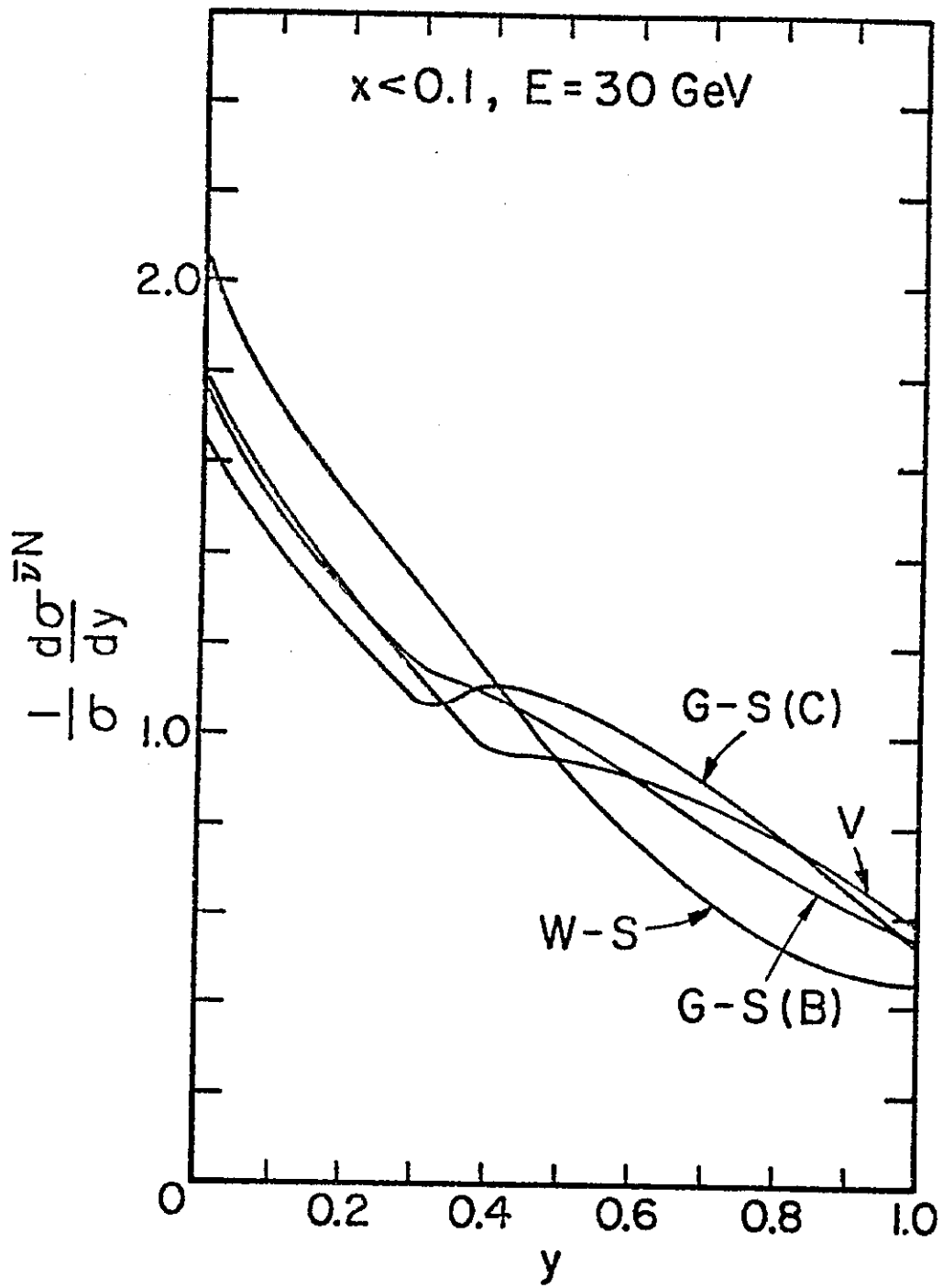


Fig. 2

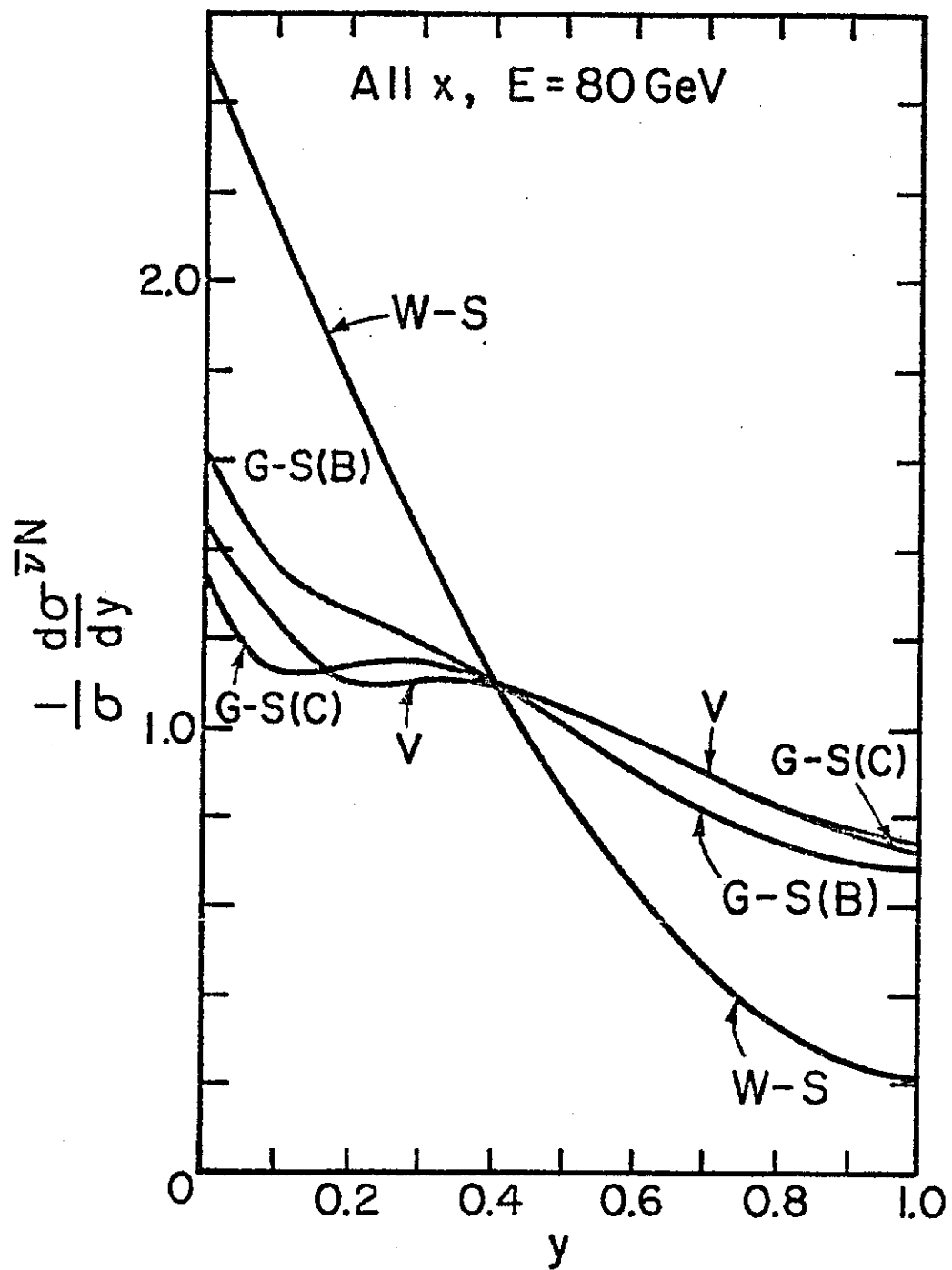


Fig. 3

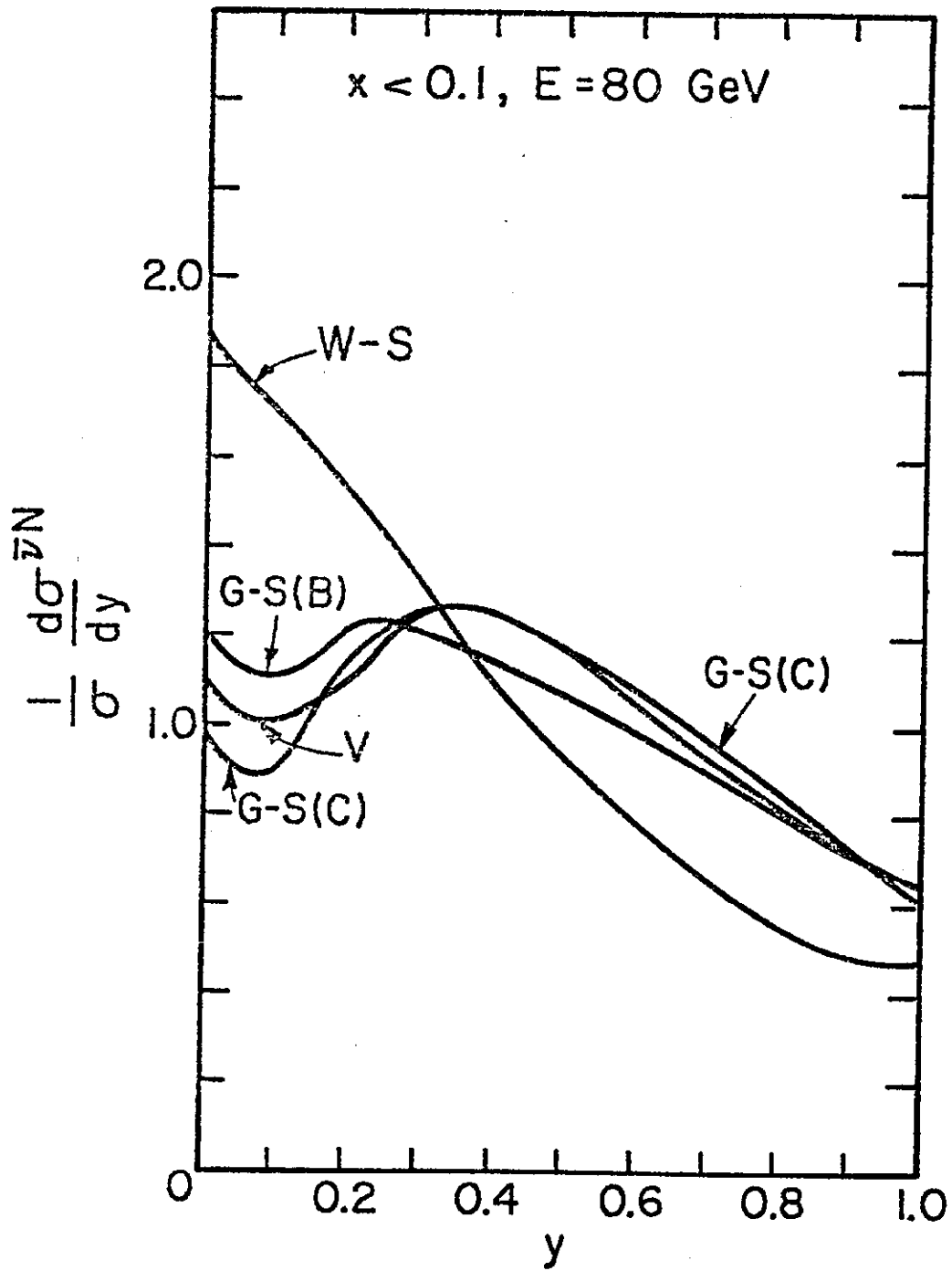


Fig. 4

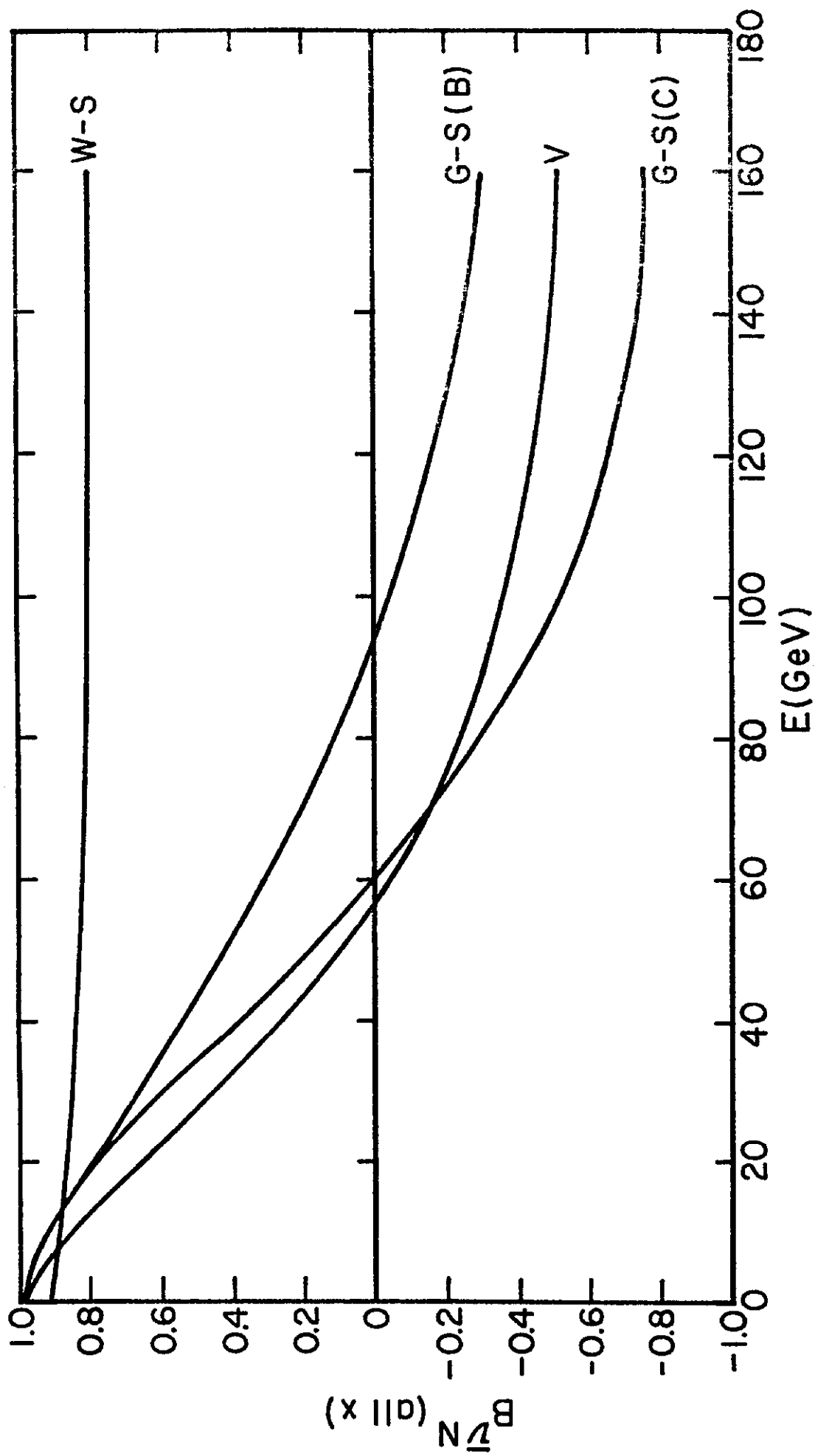


Fig. 5

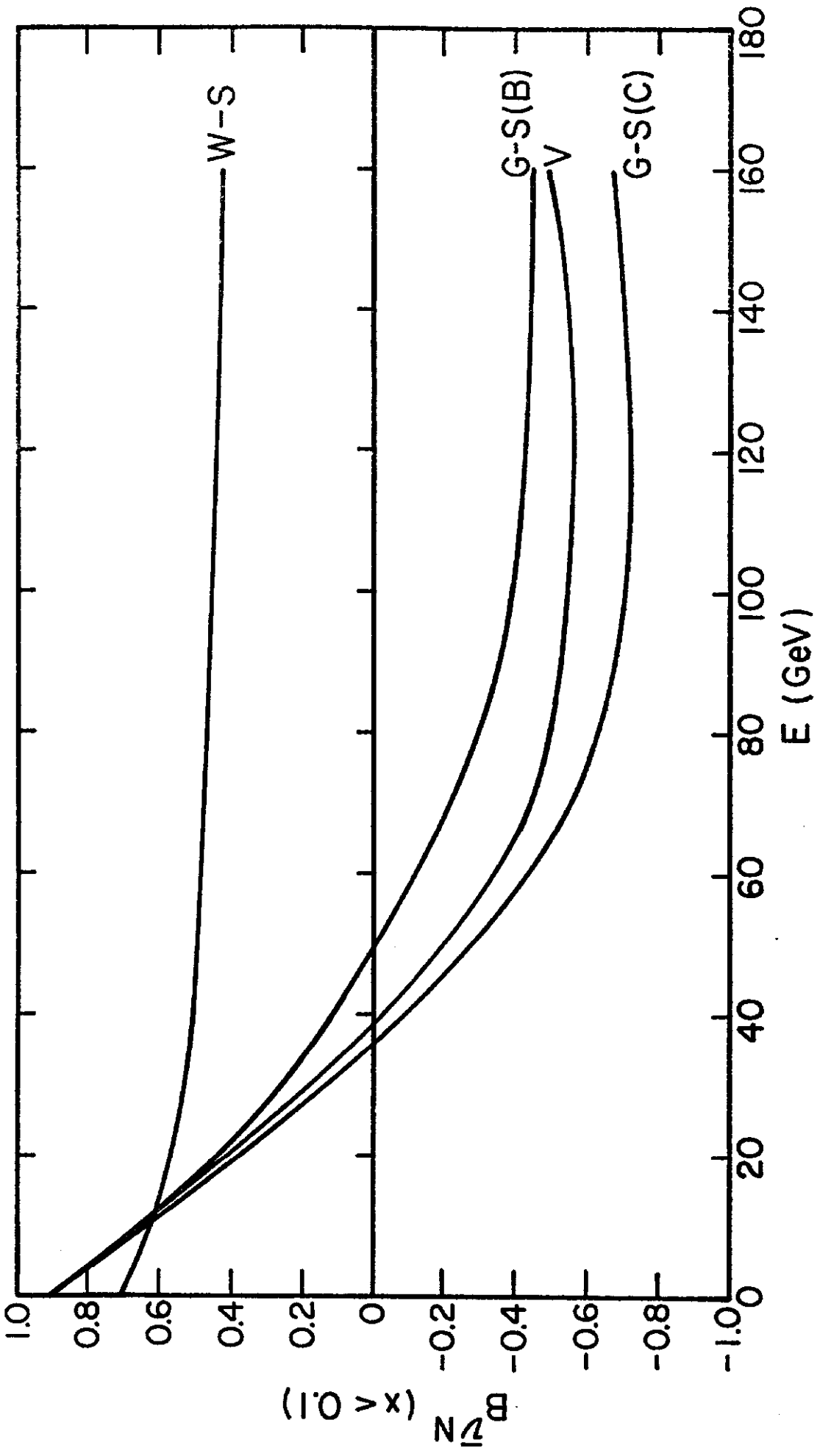


Fig. 6

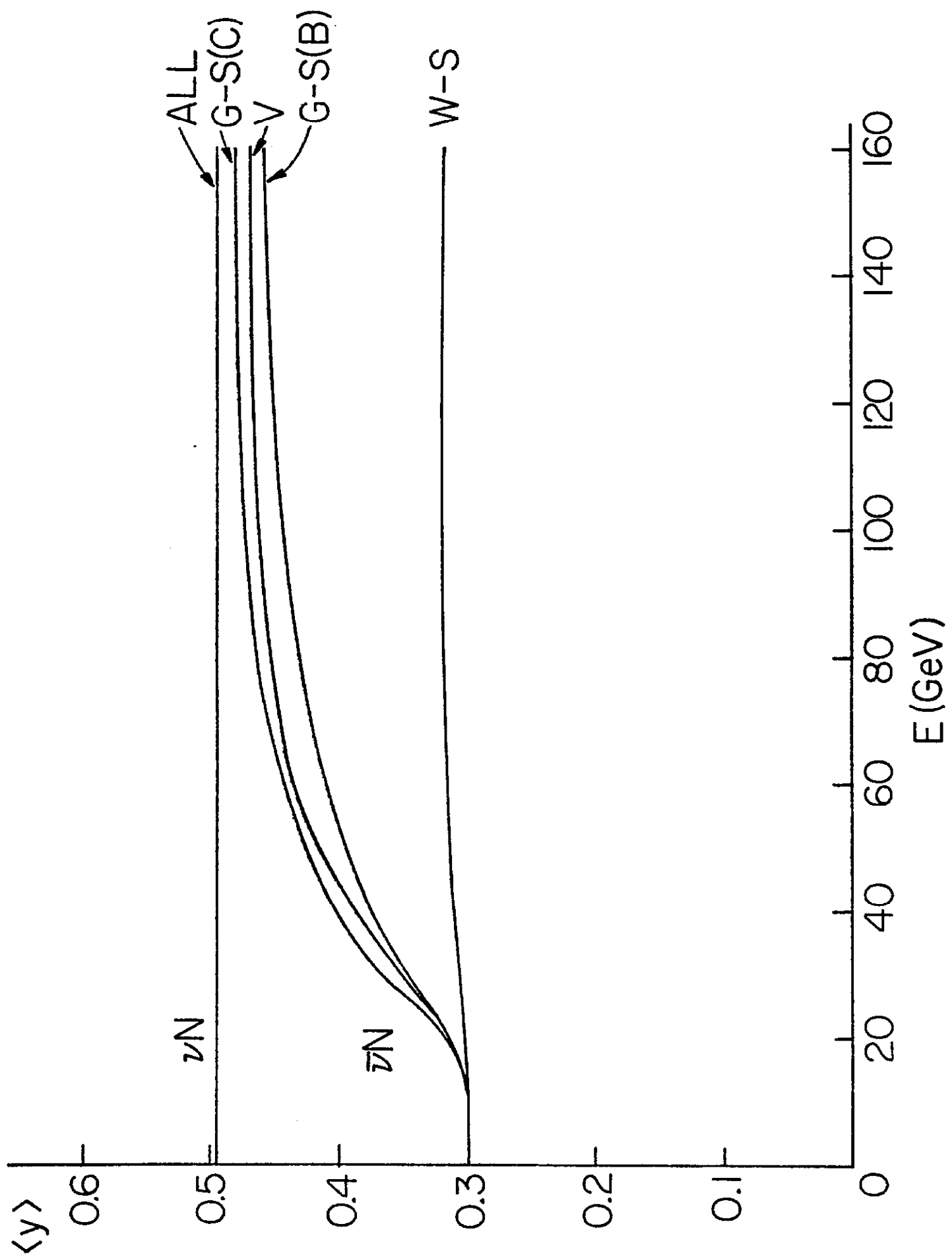


Fig. 7

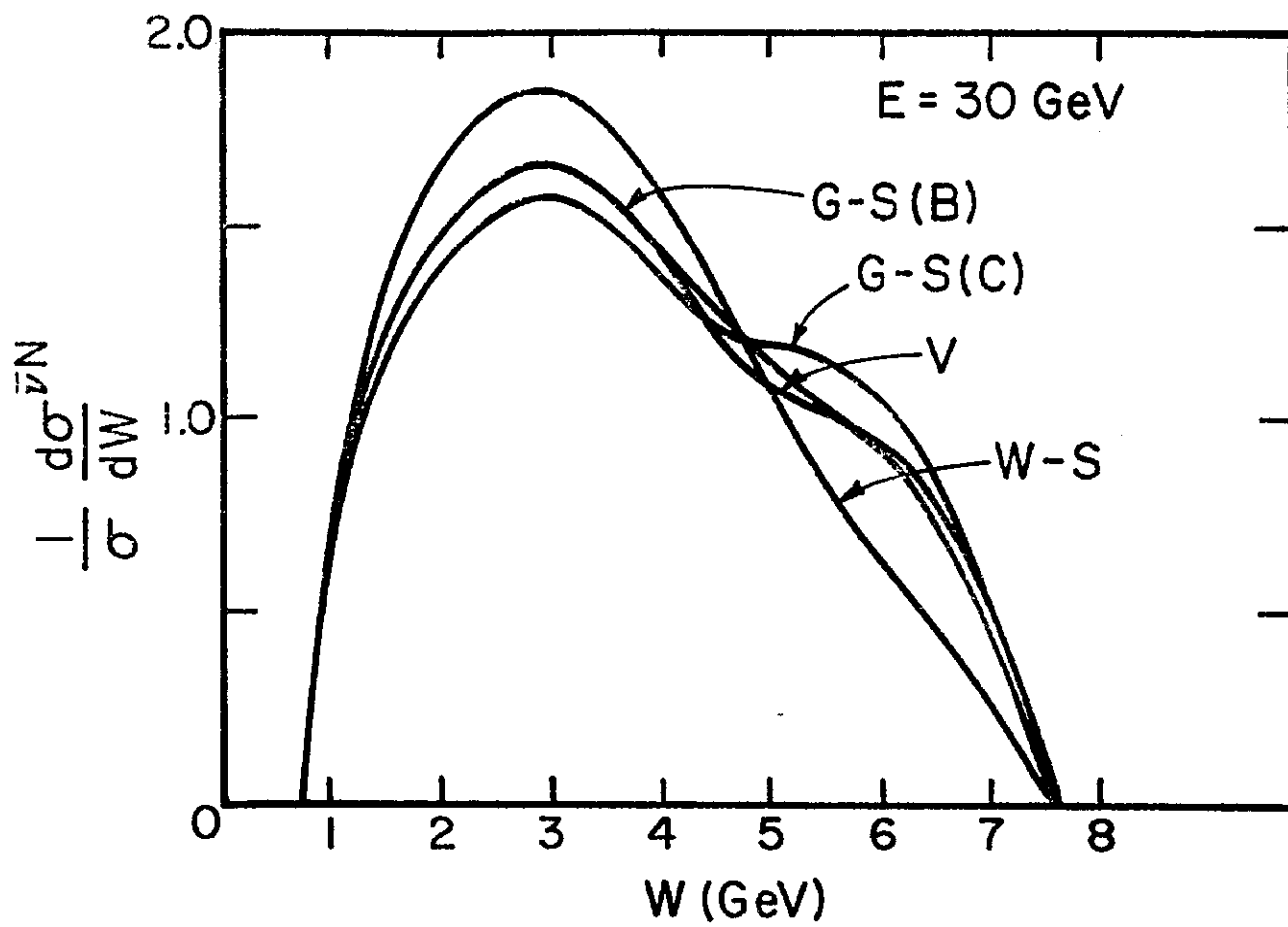


Fig. 8

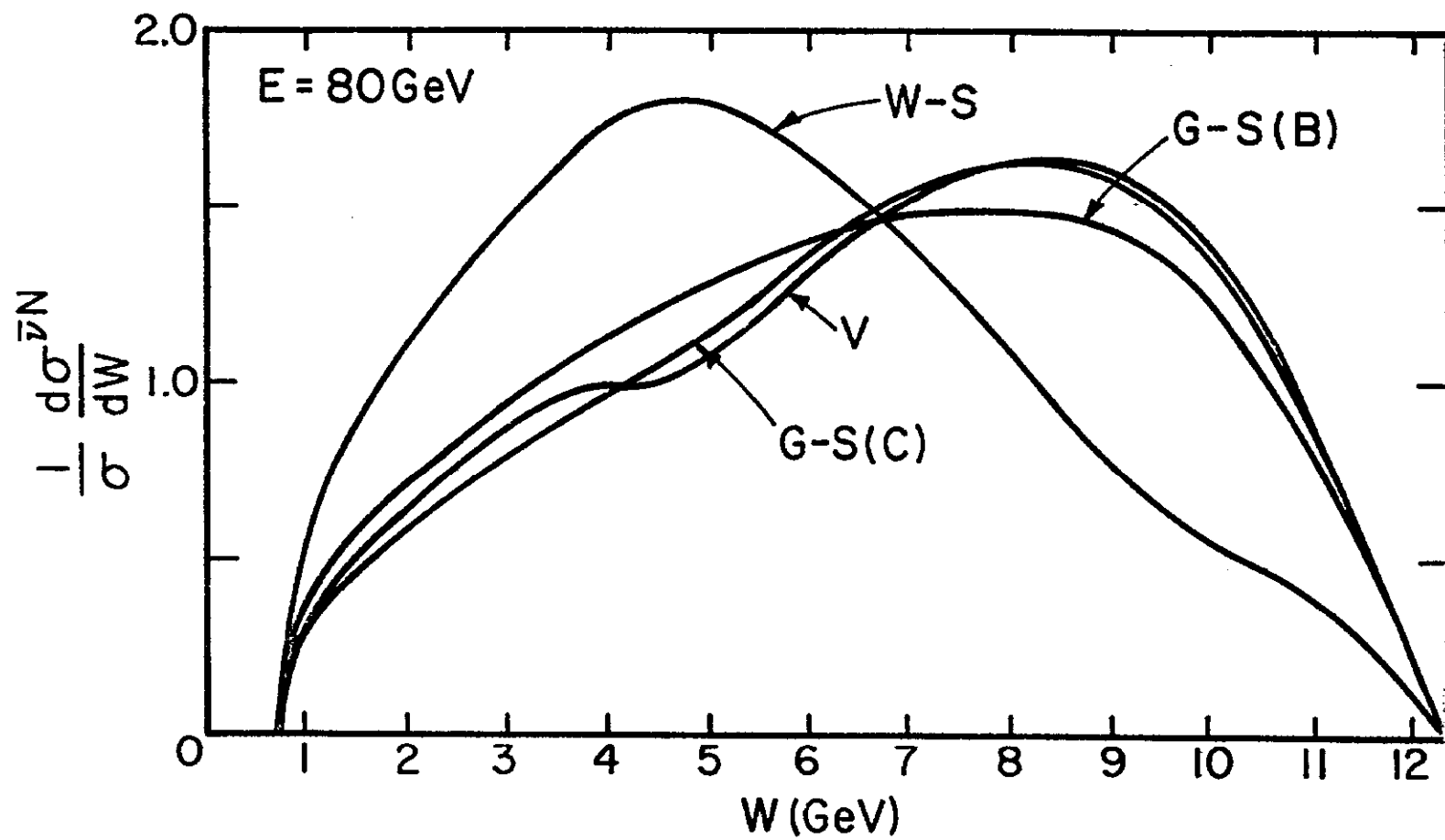


Fig. 9

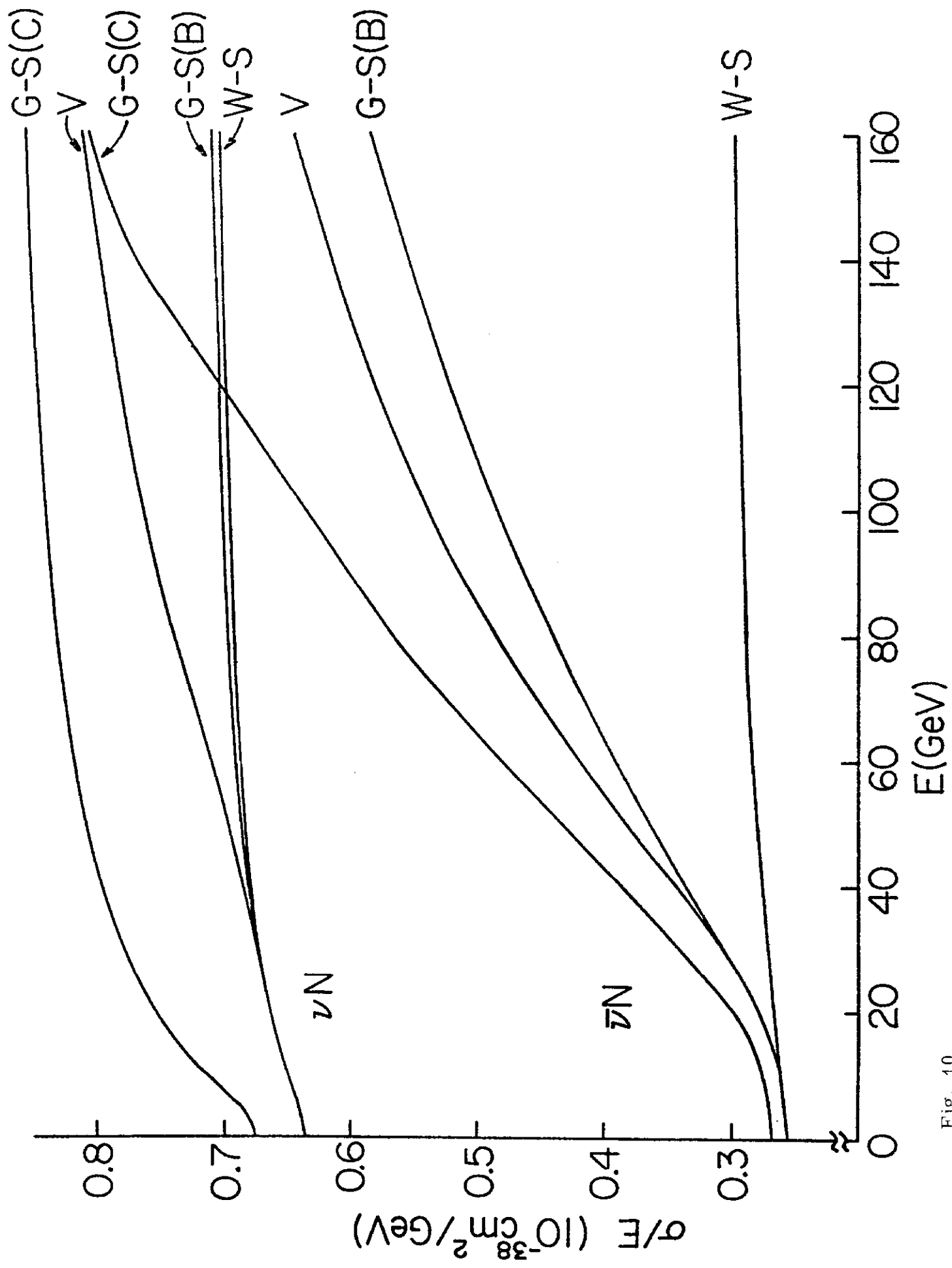


Fig. 10

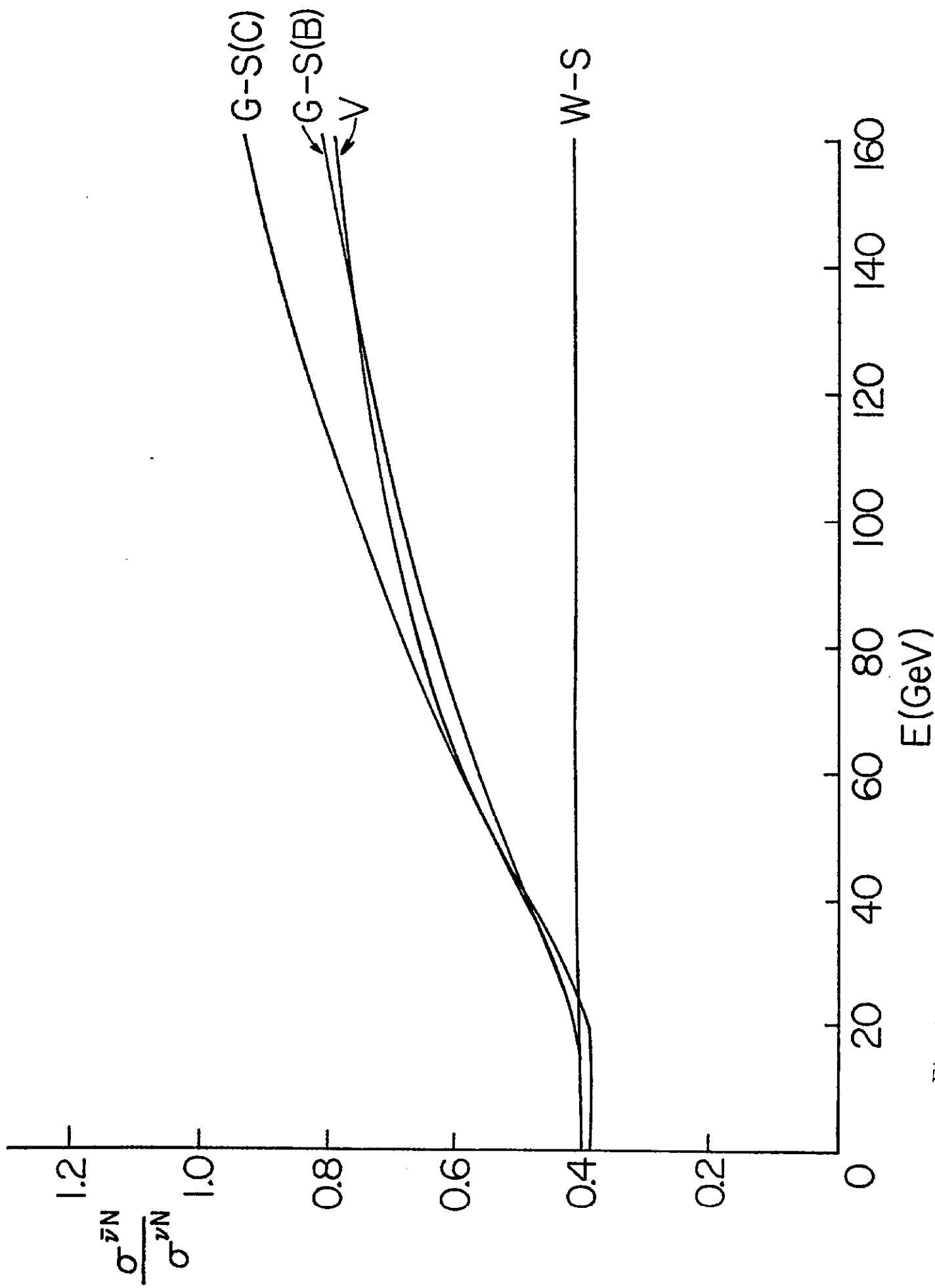


Fig. 11

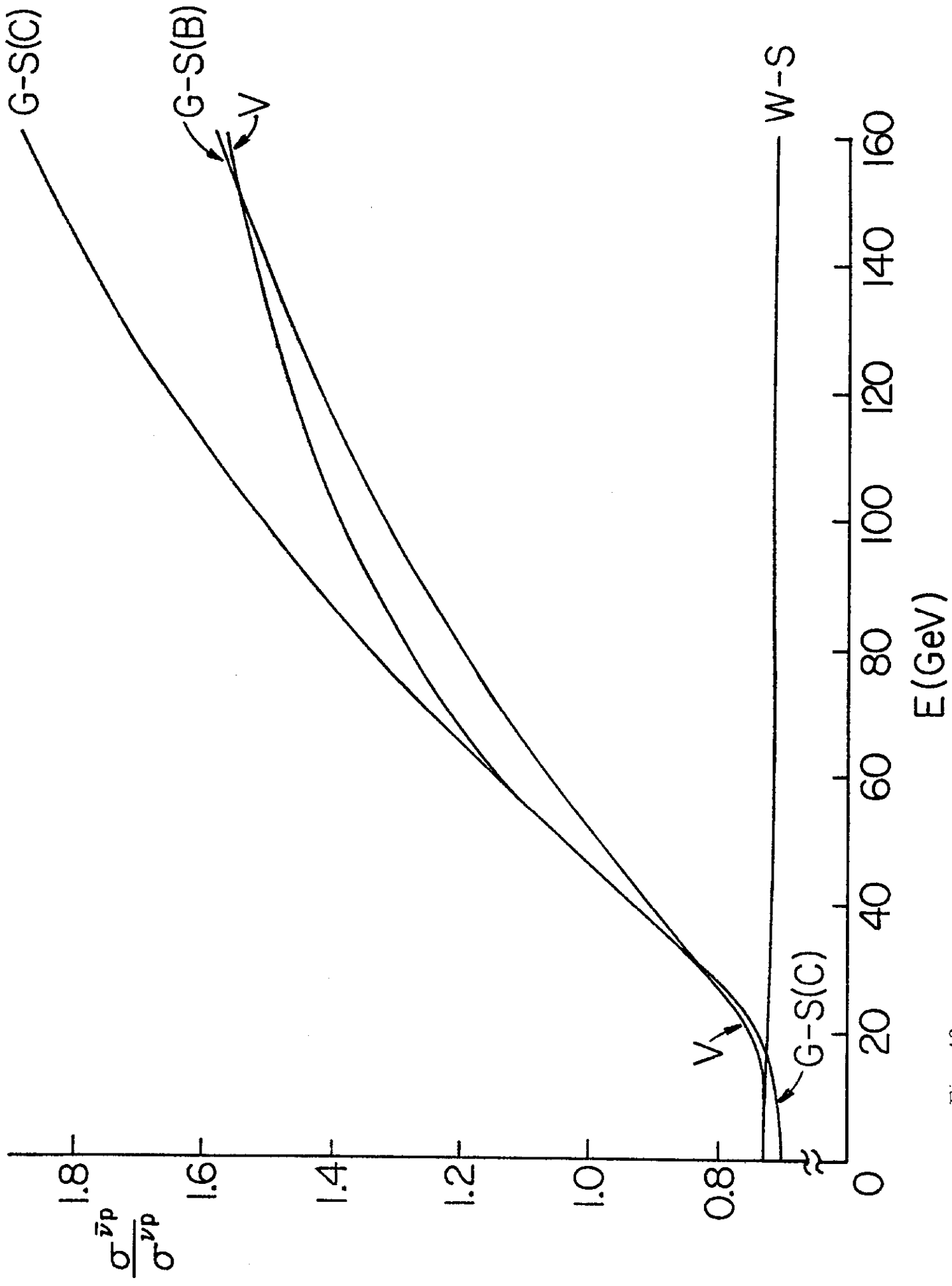


Fig. 12